Journal of Colloid and Interface Science 630 (2023) 328–340

Contents lists available at ScienceDirect

Journal of Colloid and Interface Science

journal homepage: www.elsevier.com/locate/jcis

Supramolecular structure organization and rheological properties modulate the performance of hyaluronic acid-loaded thermosensitive hydrogels as drug-delivery systems

Anderson F. Sepulveda [a,b], Mont Kumpgdee-Vollrath [c], Margareth K.K.D. Franco [d], Fabiano Yokaichiya [e,*], Daniele R. de Araujo [a,*]

[a] Human and Natural Sciences Center, Federal University of ABC, Santo André, São Paulo, Brazil
[b] Drugs and Bioactives Delivery Systems Research Group—SISLIBIO, Federal University of ABC, Santo André, São Paulo, Brazil
[c] Beuth Hochschule für Technik Berlin, Berlin, Germany
[d] Instituto de Pesquisas Energéticas e Nucleares—IPEN, São Paulo, São Paulo, Brazil
[e] Department of Physics, Federal University of Parana, Curitiba, Parana, Brazil

GRAPHICAL ABSTRACT

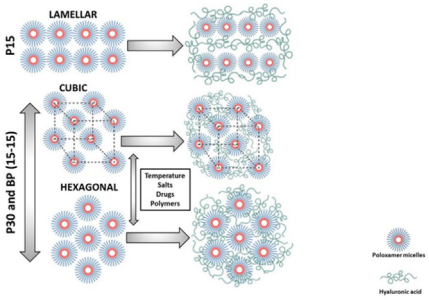

ARTICLE INFO

Article history:
Received 29 June 2022
Revised 15 September 2022
Accepted 14 October 2022
Available online 28 October 2022

Keywords:
Poloxamer
Hydrogel
Drug delivery

ABSTRACT

The challenges for developing new pharmaceutical formulations based on natural and synthetic polymers has led to innovation into the design of systems responsive environmental stimuli such as temperature. However, the presence of hydrophilic or hydrophobic molecules, charged groups, or metallic elements can affect their structural behavior and their biopharmaceutical performance This work aims to study and characterize the morphology and structure of polymeric formulations based on Poloxamer (PL) 407 (15 % and 30 % m/v) and its binary with PL 338 (15 % PL 407 + 15 % PL 338) and hyaluronic acid (0.5 % m/v), as drug delivery systems of local anesthetic bupivacaine (0.5 % m/v) and ropivacaine (0.5 % m/v) hydrochloride. For this, it was performed SANS analysis for determination of supramolecular organization and lattice parameters; calorimetry was done to characterize their thermodynamic parameters; rheological analysis flow curve, consistency and adhesion calculation, Maxwell model study. Also, it was performed drug release profiles and calculation of diffusion coefficients. It was identified lamellar structures in PL 407 15 % formulations, and coexistence of cubic and hexagonal phases in PL 407 30 % and binary formulations, however hyaluronic acid, bupivacaine or ropivacaine seem do not affect the type of supramolecular structure. In addition, these additives can modulate viscosity among poloxamers chains, increasing micelle-micelle interactions as it happens in presence of bupivacaine. On the other hand, addition of hyaluronic acid can promote increased structural stabilization by hydrophilic interactions between hyaluronic and micellar corona. It reflects the ability how to control the drug release, as in case

* Corresponding authors at: Drug and Bioactives Delivery Systems Research Group-SISLIBIO. Human and Natural Sciences Center, ABC Federal University, Santo André, SP, Brazil and Av. dos Estados 5001, Bloco A, Torre 3, Lab 503-3, Bairro Bangu, Santo André, SP CEP 090210-580, Brazil (D.R. de Araujo).
E-mail addresses: fabiano@fisica.ufpr.br (F. Yokaichiya), daniele.araujo@ufabc.edu.br (D.R. de Araujo).

https://doi.org/10.1016/j.jcis.2022.10.064

of binary system that retained bupivacaine for longer time than other systems, as well it happens when hyaluronic acid is added in PL 407 15 % and PL 407 30 %.

1. Introduction

The possibility of designing new pharmaceutical formulations based on natural and synthetic polymers has led to the development of systems that can respond to distinct stimuli such as temperature, pH gradient, chemical and light, and electrical and magnetic fields. However, the presence of hydrophilic or hydrophobic molecules, charged groups, or metallic elements can affect their structural behavior and impact the drug release rate and biopharmaceutical performance [1,2].

Poloxamers (PL) are copolymers composed of hydrophilic polyethylene oxide (PEO) and hydrophobic polypropylene oxide (PPO) blocks, represented as PEO_x-PPO_y-PEO_x (Fig. 1 A), where x and y confer different physicochemical properties and enable their interaction with hydrophilic and hydrophobic interfaces. In aqueous solutions, these copolymers self-organize into micelles at appropriate temperatures and concentrations [3–5]. With increasing temperature, micelles tend to enhance their structural order, with dehydrating PPO units organizing themselves (“packing”) into lamellar, cubic, and hexagonal phases, producing partially rigid structures with high elastic moduli [6]. This reversible phenomenon, known as gelation, is characterized by the temperature (or temperature range) of sol–gel transition (Tsol-gel), as they remain fluid or viscoelastic semi-solid gels depending on the environmental temperature [7,8].

Over the last two decades, studies on PL-based binary systems (for example, PL407 + PL338) as drug-delivery matrixes have accumulated; however, controversies regarding the supramolecular structure and interference of drug incorporation and other additives (as different polymers) persist, along with how they impact biopharmaceutical properties of pre-formulations. Indeed, these critical questions need to be resolved, as interferences between the copolymer concentration and temperature are necessary for micellization processes and gelation in binary systems, an alternative strategy to modulate the micellar structure, hydrogel rheological properties, formulation stability over physical condition changes, solubility, and drug release rate [2,6,9]. Having said that, we investigated the binary systems phase behavior composed of two hydrophilic PL, PL407 and PL338. Despite their structural similarities, both polymers show some differences regarding to molecular weight, ethylene oxide (EO): propylene oxide (PO) relationships and CMC (Fig. 1), which determines their differential phase organization behavior and supramolecular organization according to their final concentration and ratio into the formulation. Other important point is their potential low cytotoxicity, justifying their selection as hydrogels matrices [9,10].

Previous studies have discussed interactions between PL and natural polymers [10–12]. However, establishing how additive incorporation can impact hydrogel phase organization could, in turn, determine the structural requirements for modulating their release rates and mechanisms [7,9]. Conversely, negative charges and hydroxyl groups in hyaluronic acid (HA) chains at physiological pH afford the HA molecule hydrophilic characteristics (Fig. 1 B). In addition, its high molar mass confers unique viscoelastic and rheological properties [10,13,14]. We have previously reported the influence of low HA concentrations on the PL407-PL338 hydrogel matrix for intra-articular applications; however, the drug model used, lidocaine base, also had a differential function in structural changes [9].

Herein, we investigated two chemically related amino-amide local anesthetics, bupivacaine hydrochloride (BVC) and ropivacaine hydrochloride (RVC), widely used for intraoperative and postoper-

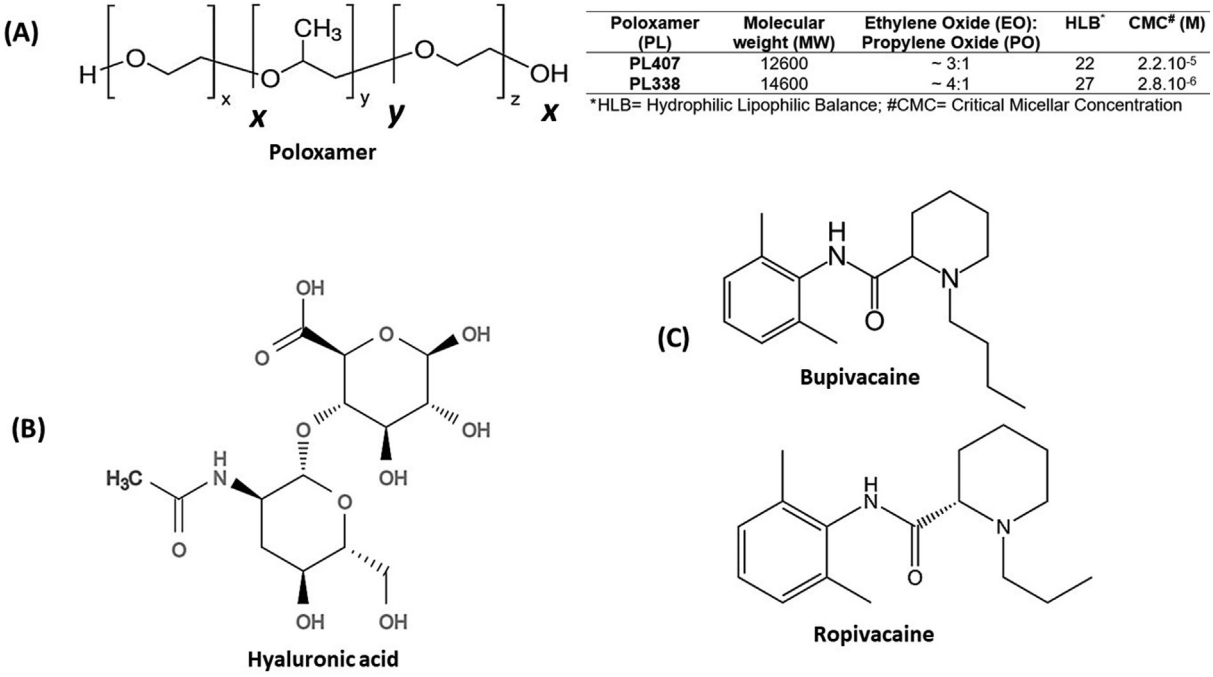

Poloxamer (PL)	Molecular weight (MW)	Ethylene Oxide (EO): Propylene Oxide (PO)	HLB*	CMC# (M)
PL407	12600	~ 3:1	22	$2.2.10^{-5}$
PL338	14600	~ 4:1	27	$2.8.10^{-6}$

*HLB= Hydrophilic Lipophilic Balance; #CMC= Critical Micellar Concentration

Fig. 1. Chemical structures of (A) Poloxamer (PL), (B) hyaluronic acid (HA), and (C) drugs; bupivacaine (BVC) and ropivacaine (RVC).

ative pain relief (Fig. 1 C). BVC is more hydrophobic than RVC, mainly due to the butyl group in its chemical structure, whereas RVC presents a propyl radical. This primary chemical difference determines their mechanism of action mediated by blocking sodium channels, the duration of anesthetic effects, and cardiac toxicity [1]. Although both drugs have been investigated in several nanocarrier systems, in the present report, we aimed to present a physico-chemical look at how the molecular study of drug and hydrogel component interactions should also be explored from an active drug role perspective, considering their chemical structure and availability as salt forms. We synthesized HA-loaded PL hydrogels containing BVC or RVC and performed small-angle neutron scattering (SANS), differential scanning calorimetry (DSC), and rheological property examinations to determine viscoelasticity, flow resistance, adhesion, and cohesion, as well as their release profiles.

2. Materials and methods

2.1. Excipients, drugs and salts

Poloxamers 407 and 338 (Sigma-Aldrich, Chem. Corp. Saint Luis, MO, USA), and HA (98.5 % purity, 150 kDa; Viafarma Ind. Farmc., São Paulo, Brazil) were used as excipients. BVC and RVC (hydrochloride form) were a gift from Cristália Produtos Químicos Farmacêuticos LTDA (Itapira, São Paulo, Brazil). Sodium chloride, monobasic phosphate, and basic salts were purchased from Sigma-Aldrich Chem. Corp (Saint Luis, MO, USA). All other chemicals were of analytical grade.

2.2. Hydrogel preparation

Each sample was carefully prepared by weighting appropriate amounts of each PL considering 15 to 30 g / 100 mL (m/v) for PL407 or PL338 as unique or binary systems. All samples were prepared in ultrapure water and kept under constant magnetic stirring (300 rpm) in ice bath until complete dissolution and transparency. Polymeric solutions were then stored overnight at 8 °C until convenient use. For preparation of samples in deuterated water, were used 2 mL of D_2O to reduce the incoherent scattering produced by hydrogen [15], for rheological analysis, and 10 mL for SANS analysis.

2.3. SANS

The SANS experiments were performed at Helmholtz-Zentrum Berlin für Materialien und Energie-Berlin (HZB, Berlin, Germany) using a V16 (VSANS) instrument. Data were obtained in a two-dimensional detector at two different distances: (a) 1.7 m with wavelengths from 1.8 Å to 3.8 Å and (b) 11 m with wavelengths from 1.6 Å to 9.2 Å. The results were added and averaged radially in the range of q from 0.006 to 0.5 $Å^{-1}$. The samples were measured at temperature intervals from 20 to 50 °C. To ensure temperature stability and homogeneity of samples, a waiting time of 30 min was used. Data were normalized by detector background, empty sample holder, and detector efficiency and were scaled to absolute intensities using standard measurements of 1 mm H_2O. The solvent backgrounds were corrected for each SANS measurement. All structures were determined by Micellar Supramolecular Structure Software (MiSS), developed by our group (registered at Brazilian Institute of Industrial Property, BR 51 2021 000746-8).

To analyze the structural orientational order of hydrogels, 2D SANS patterns, 0.07175 $Å^{-1}$ < q < 0.556894 $Å^{-1}$, were converted to intensity profiles as a function of azimuthal angle $I(\theta)$, assuming uniaxial symmetry [16,17], using SasView 5.0.4 software. Azimuthal plots were then fitted by the Gaussian model. From the second-order Legendre polynomial, the order parameter S is defined as (Eq. (1)):

$$S = \frac{3}{2}\frac{\int_0^{2\pi} \exp\left\{-(\theta-\theta_c)^2/2\sigma^2\right\} \sin\theta cos^2\theta d\theta}{\int_0^{2\pi} \exp\left\{-(\theta-\theta_c)^2/2\sigma^2\right\} \sin\theta d\theta} - \frac{1}{2} \quad (1)$$

2.4. Differential scanning calorimetry (DSC)

All DSC analyses were performed using a Netzsch DSC Polyma calorimeter (Netzsch, Selb, Germany). The hydrogel samples were weighed in aluminum pans and analyzed under three cooling-heating cycles (5 °C/min. ratio) as follows: 1) heating from 0 to 50 °C (cycle 1); 2) cooling from 50 to 0 °C (cycle 2); 3) heating from 0 to 50 °C (cycle 3). All analyzes were performed in triplicate, and the thermograms are represented by heat flow (cal/g. s) as a function of the temperature (°C).

2.5. Rheological analysis

Rheological analyses were performed using an oscillatory rheometer with cone-plate geometry (KinexusLab, Malvern Instruments, Malvern, UK) at temperatures from 10 to 50 °C, a shear strain of 1 %, and a frequency of 1 Hz for obtaining values of elastic modulus ($G\prime$) and viscous modulus ($G\prime\prime$). Oscillatory scanning analyses were performed at 37 °C and 0.1 to 10 Hz. Rheological data modeling was obtained considering the frequency values, and this range was converted to rad/s using the relation $\omega = 2\pi f$. Each analysis was performed in triplicate for each formulation.

For all formulations, plots of $G', G\prime\prime(T)$ and $\eta(T)$ were plotted to analyze viscoelastic behavior. To obtain the gelation temperature, $T_{sol-gel}$, the Boltzmann sigmoidal function was fitted to the viscosity plot, $\eta(T)$ [18] (Eq. (2)):

$$\eta(T) = \eta(0) + \frac{\eta_{max} - \eta(0)}{1 + exp\left(\frac{T_{sol-gel}-T}{v}\right)} \quad (2)$$

where $\eta(0)$ is the lowest viscosity measure, η_{max} is the highest viscosity measure, and v is defined in Eq. (3) as follows:

$$v = \frac{d}{dT}\eta(T) \quad (3)$$

G' as a function of frequency ω typically follows the power-law model described by Eq. (4):

$$G' = A \cdot \omega^n \quad (4)$$

where A is related to adhesion property and n is the viscoelastic exponent.

Adhesion is defined as a property that is proportional to the force required to remove material from a surface. This model is ideal for studying the relationship between the formulation used, the environment in which the formulation is applied, and the strength of this interaction [19]. Some polymeric solutions can be modeled as a spring-dashpot system because chains can respond to an applied force and return to their previous state as an elastic component [20,21]. According to this model, the elastic component (spring) is serially connected to the viscous component (dashpot). Chain elasticity is dependent on the entanglements among polymeric chains, in addition to the hydrophilic and hydrophobic effects, which can be modeled based on the Maxwell model described in (Eqs. (5) and (6)):

$$G'(\omega) = \frac{G_\infty(\tau\omega)^2}{1+(\tau\omega)^2} \quad (5)$$

$$G''(\omega) = \frac{G_\infty \tau\omega}{1 + (\tau\omega)^2} \quad (6)$$

where τ is the relaxation time (or reciprocal of the chain-end disengagement rate). Based on the Green and Tobolosky theory [22] for transient networks, G_∞ is proportional to the number density of the effective temperature-dependent elastic chains. As G_∞ is related to G', the polymer concentration critically impacts enhanced entanglement [20,21].

To determine the flow curves of all formulations, we used a range of shear rates γ between 0 and 100 s^{-1}. All curve flows were obtained at 25 °C and analyzed using the power-law model (Eq. (7)):

$$\sigma = K \cdot \gamma^m \quad (7)$$

where K is related to the formulation consistency and m is the flow or consistency index. For hydrogel systems, $m < 1.0$ was expected due to its shear-thinning quality.

2.6. In vitro release profiles and elucidation of release mechanisms

In vitro release tests were performed using a membraneless model to simulate contact between the sample and biological fluids, as described in our previous study [23]. Briefly, hydrogel samples (1 mL) were placed in a donor compartment, while the receptor compartment was filled with 25 mL of sodium phosphate buffer (5 mM) and sodium chloride (154 mM) at pH 7.4 and 37 °C under magnetic stirring at 100 rpm. Aliquots (1 mL) were withdrawn at intervals of 30 min, 1, 2, 4, 5, 6, 7, and 24 h, and the same volume was replaced by sodium phosphate buffer (5 mM, with 154 mM NaCl, pH 7.4). Aliquots were analyzed by UV − Vis spectrophotometry according to previously determined analytical curves (λ = 263 nm, y = 0.08656 + 0.001323x, R^2 = 0.9778; y = 0.1075 + 0.001234x, R^2 = 0.9980 for BVC and RVC, respectively).

To determine the drug release mechanisms of different formulations, zero-order, Higuchi, and Korsmeyer-Peppas mathematical models were applied [24], as described below (Eqs. (8), 9 and 10):

$$Q(t) = Q_0 + K_0 t \quad (8)$$

where Q is the amount of drug released at time t, Q_0 is the initial drug amount, and K_0 is the zero-order release constant.

$$Q(t) = K_H \sqrt{t} \quad (9)$$

where K_H is the release coefficient, and.

$$\frac{M(t)}{M_\infty} = K_{KP} t^n \quad (10)$$

where $M(t)/M_\infty$ is the drug released fraction at time t. K_{KP} is a rate constant, and n is the release index. The release obeys Fickian diffusion when the value of n is 0.45. When $0.45 < n < 0.89$, it obeys non-Fickian or anomalous diffusion; it obeys case-II transport when n = 0.89 and super case-II transport when > 0.89. Data were adjusted using linear regression, and the determination coefficient (R^2) was assessed.

In addition, the drug transference rate was determined considering a diffusional parameter as a function of the square root of time, as described by Equation (11):

$$\frac{M(t)}{M_\infty} = \beta \frac{\sqrt{Dt}}{h\sqrt{\pi}} \quad (11)$$

where $M(t)$ is the amount of drug released at time t, M_∞ is the initial amount of drug, D is the diffusion coefficient in the system, t is the time, and h is the thickness of the hydrogel in the donor compartment. The coefficient β is dependent on the ratio C_0/C_s, where C_0 is the initial concentration of the drug in the donor compartment and C_s is the solubility of the drug in the hydrogel [25].

2.7. Statistical analysis

Data from rheological analysis and SANS parameters are represented as mean ± standard deviation and correlation coefficient (R^2). Drug release profiles were analyzed using a one-way analysis of variance (one-way ANOVA), followed by the Tukey-Kramer test or two-tailed unpaired t-test. All data were analyzed using Graph Pad Prism (Graph Pad Software Inc., USA), and rheological results were analyzed using rSpace software for Kinexus®. Statistical significance was defined as $p < 0.05$.

3. Results and discussion

3.1. SANS analysis: supramolecular structure of hydrogel is differentially influenced by BVC, RVC, and HA

The structural study of polymeric hydrogels is an important strategy for determining their biopharmaceutical properties and establishing relationships with their biological functions. Studies assessing hydrogel structural organization using SANS have shown promising results in terms of understanding interactions between their components and the influence of additives (such as drugs) on formed structures [26–28].

Comparisons between PL concentrations and isolated and binary systems showed that PL407 15 % samples exhibited a lamellar structure, typically observed in hydrogels with low PL final concentrations [15,29]. However, cubic and hexagonal structures coexisted in the PL407 30 % system, as well as in the binary system (PL407 15 % + PL338 15 %). Previous studies have reported the predominance of hexagonal structures in 30 % PL, along with cubic structures at high PL concentrations [6,29,30], to minimize osmotic constraints [29,30].

The total PL concentration is an important component for defining the supramolecular organization [6]. Moreover, the chemical characteristics of each component are responsible for this internal organization and, consequently, particle dimensions. BVC, RVC, and HA are known to affect the structure of 15 and 30 % PL407 hydrogels. In addition, the incorporation of both drugs seems do not affect the structural size of P15 formulations, although it seen that hyaluronic acid can be more sensitive to bupivacaine presence: P15 + HA (from ∼ 19.3 nm in P15 + HA to 21 nm in P15 + HA + BVC). The lattice parameter decreased into both cubic and hexagonal structures on adding P30 (Table S1).

Conversely, the binary system BP 407–338 was more stable to changes, considering both temperature and the presence of additives, despite exhibiting a lower viscosity than P30 systems. A possible reason for this characteristic is the formation of a mixed hydrogel structure, although both polymers possess different molecular masses and hydrophilicities [31].

As shown in Fig. 2 and Table S2, the intensity peaks are slightly shifted from theoretically expected positions, given the presence of additives [7,15]. The shoulder observed at ∼ 0.4 Å coincides with the expected peak for the cubic structure; however, this wide peak is caused by the possible formation of polymer-drug clusters in samples.

For P30 hydrogels, different phase organizations coexist, with both Fm^3m cubic and hexagonal structures identified. No structural differences were observed at 25 and 37 °C (Table S1), as the systems were in a gel state, organized such that the lattice parameters were unaltered over this short temperature range. Indeed, P30 samples were more sensitive to the presence of RVC than BVC (Fig. 2B, E), given that RVC tends to influence the systems at high temperatures, causing a disturbance in micelle-micelle interactions. In contrast, this effect was not observed in the presence of

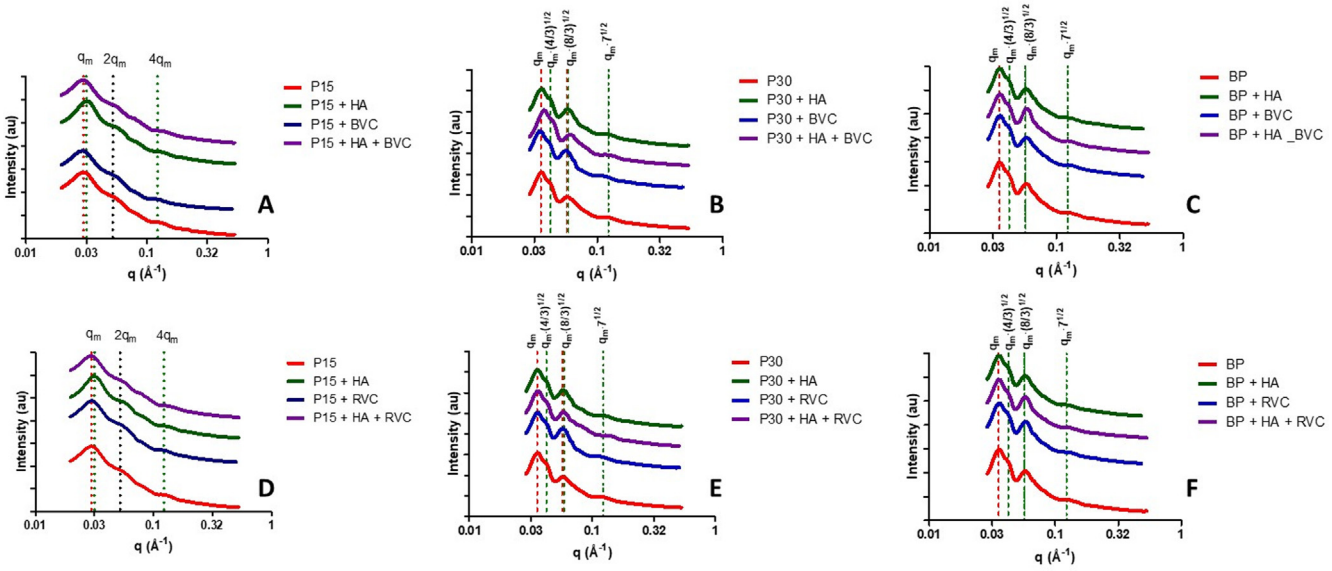

Fig. 2. Intensity profiles of PL 407 15 % (P15, graphs A, D), PL 407 30 % (P30, graphs B, E), and PL 407 15 % + PL 338 15 % (BP, graphs C, F) formulations, with hyaluronic acid (HA), bupivacaine (BVC), and ropivacaine (RVC), obtained from SANS measurements at 37 °C. It is observed lamellar structures in all P15 formulations (with reflections at qm, 2qm and 4qm). There is coexistence of phases in P30 and BP systems, with Fm3m cubic (–), (with reflections at qm, √(4/3) qm, √(8/3) qm) and hexagonal supramolecular structures (-.-) (with reflections at qm, √3 qm, √7 qm). For clarity, identification of the peaks are shown on Table S2.

HA, suggesting the potential interaction with the hydrophilic corona in intermicellar spaces.

Similarly, Nascimento et al. [9] have shown that PL407 20 % exhibits lamellar supramolecular organization, although it tends to become hexagonal in the presence of lidocaine or HA (0.025 and 0.05 % m/v) at 37 °C. Additionally, both HA concentrations helped stabilize these hexagonal structures by interacting with the micellar corona and intermicellar spaces. However, in PL338 20 % and binary PL407 10 % + PL338 10 %, HA incorporation of HA did not alter the supramolecular structure (body-centered cubic for PL 338 20 % and lamellar for PL407 10 % + PL338 10 %). Although we noted the coexistence of cubic and hexagonal structures in PL407 15 % +PL338 15 % (Fig. 2C, F), the presence of HA favored structural stabilization via hydrophilic interactions between hydroxyl groups of HA chains and the PEO portion of PL. Furthermore, we identified that both BVC and RVC did not alter supramolecular type in P15, P30, and BP formulations, although Nascimento et al. [9] have reported that lidocaine modified the system from a lamellar to hexagonal structure with PL407 20 %, and from lamellar to cubic structure in PL407 10 % + PL338 10 %. This may be attributed to the low polymer concentration, which can be more easily aggregated than in a higher concentration system.

Binary formulations seem to be structurally more stable than other hydrogels, given that temperature variation and additive incorporation did not significantly alter their structural organization. Although BP formulations contain PL 338, a more hydrophilic poloxamer than PL407 (because the PEO:PPO ratio of PL 407 is 3:1, while for PL338, the ratio is 5:1, reflecting the higher hydrophilic-lipophilic balance of PL338 than PL407), the size of the BP micelles displayed dimensions approximating the PL407 30 % systems (∼30 nm for cubic and ∼ 18 nm for hexagonal structures), suggesting the formation of a mixed system (Table S1).

All formulations presented low orientational order (ranging between S = 0.14 and S = 0.40) at both tested temperatures, although S was slightly increased under high polymer concentrations (S = 0.20 ± 0.05 in P15, S = 0.31 ± 0.07 in P30, and S = 0.20 ± 0.06 in BP), but was unaltered by temperature (Fig. 3). In P30 + BVC and P30 + RVC formulations, S values were reduced (S = 0.24 ± 0.05 in P30 + BVC, and S = 0.27 ± 0.05 in P30 + RVC), demonstrating a disturbance in the organization of all components, which indicates that water molecules were expelled from the PL structure due to the presence of the drug in a salt form (hydrochloride form), acting as structure retractor. This effect could also explain the increased viscosity, especially in the presence of BVC, as it is more hydrophobic than RVC.

In contrast, the opposite occurred when BVC or RVC was incorporated into BP. The orientational order in BP + BVC (S = 0.34 ± 0.06) and BP + RVC (S = 0.22 ± 0.06) was increased when compared with systems composed of only one PL type. These effects suggested that the presence of PL 338 plays a role in the final system organization and in improving the matriX arrangement. The addition of HA tends to fix S at 0.21 in the P15, P30, and BP samples, indicating that HA acts as a linker among the PL structures, confirming their possible chain location in the intermicellar spaces. However, the presence of BVC or RVC augmented S in the P30 + HA and BP + HA formulations, owing to enhanced HA-water interactions (Table S1). Based on these observations, a structural organization model is displayed in Fig. 4.

3.2. DSC assays: Drugs and HA maintained thermosensitive properties of hydrogels

Table 1 shows the results obtained from the thermodynamic analysis of all hydrogel formulations. In general, neither HA nor drugs can markedly impact PL-based systems and, consequently, their thermosensitive properties [9,32], maintaining micellization as an endothermic process. At high polymer concentrations (e.g., 30 % m/v), the micellization temperature decreased almost 50 % in PL30 samples when compared with PL15, with values ranging from 19 to 10 °C, which was in line with previous studies [33,34]. Binary systems have slightly higher micellization temperatures (T_m) than P30 samples, resulting in lower enthalpy values for BP samples than those observed for P15 and P30 samples, probably attributed to structural disorganization in the presence of PL 338 owing to its more hydrophilic character than PL 407. Enthalpy variation is a measure of system complexity. According to previous studies [9,35], polymer concentration and drug incorporation can influence the enthalpy values of each system. The analysis of ther-

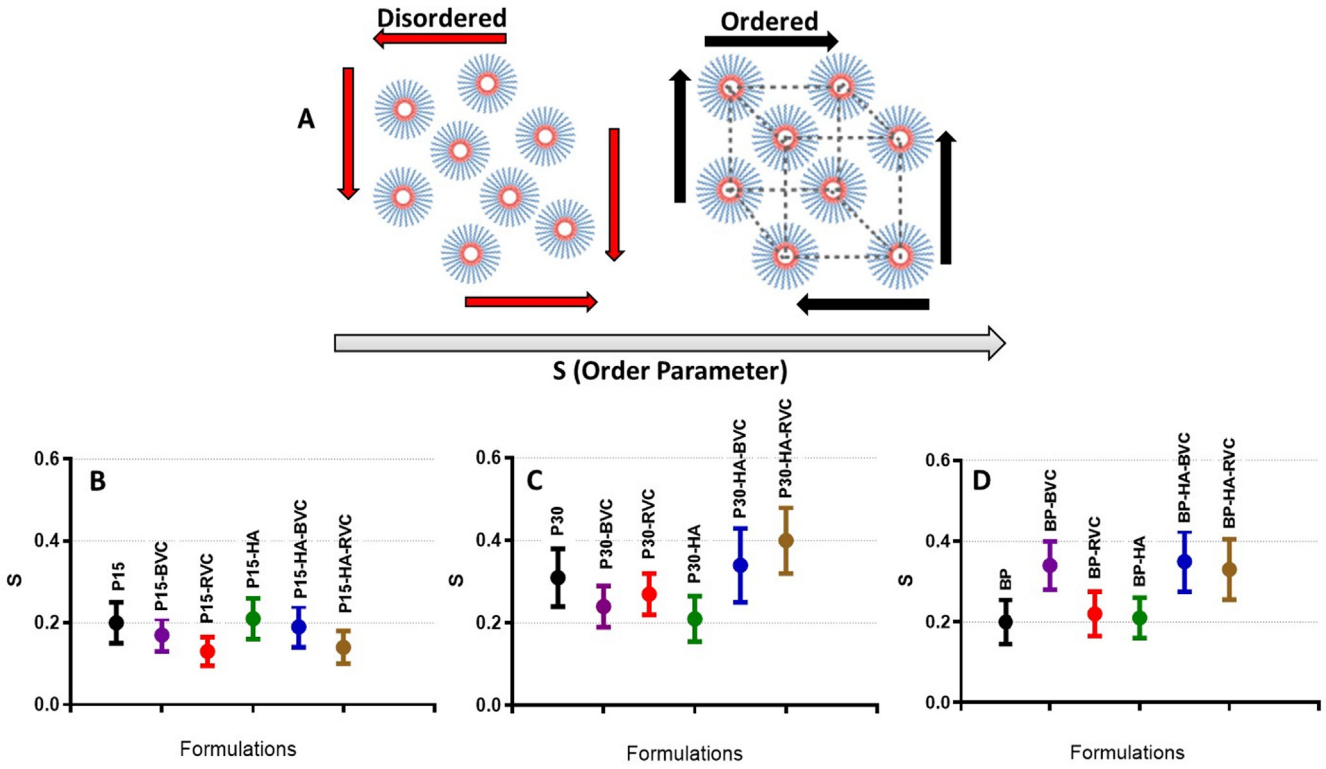

Fig. 3. (A) Scheme of orientational order parameter S: As increasing order parameter S, more organized in such orientation the material is. 2D scattering images were converted in intensity I as function of azimuthal angle, which is fitted with a Gaussian where θ_c and σ are used to calculate S. (B) S values of all P15, P30 (C) and BP (D) samples, at 25 °C, are shown.

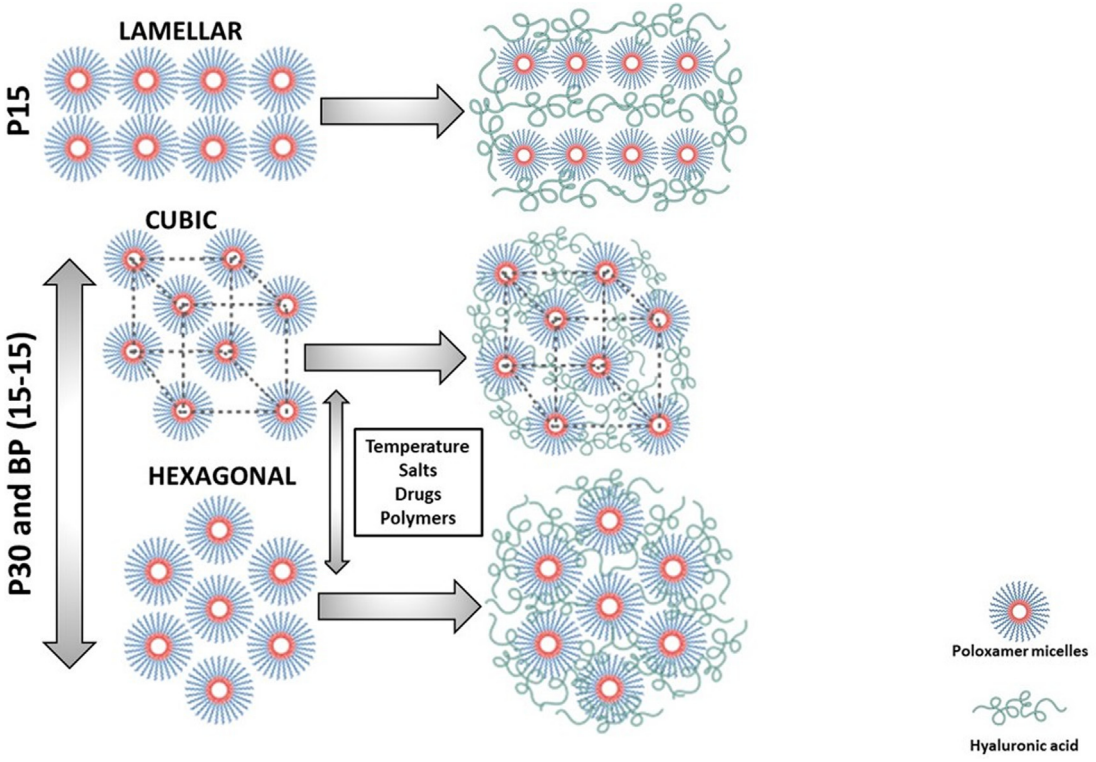

Fig. 4. Proposed model for formulations of PL 407 at 15 % and 30 %, and binary PL 407 + PL 338 at 15 % / 15 %. As shown by the SANS results, lamellar structures are observed at low poloxamer concentration. However, with the increase in the total concentration of PL, greater structuring of the formulations is promoted with the coexistence of cubic and hexagonal phases. The addition of hyaluronic acid (HA) is not able to change the type of supramolecular organization, but it does modify the rheological properties and the form of the release of bupivacaine and ropivacaine.

Table 1
Thermodynamic and rheological parameters for P15, P30 and BP hydrogels.

Formulation (% m/v)	**Additives**	T_m (°C)	ΔH(kJ mol^{-1})	$T_{sol\text{-}gel}$ (°C)	$d\eta/dT$(Pa s /°C)	G'/G"	η (Pa s)
15		18.6	38.8	45.5 ± 0.02	1.3 ± 0.02	0.18	0.30
	BVC	17.9	40.6	43.3 ± 0.07	2.00 ± 0.05	0.16	0.77
	RVC	18.2	39.0	24.8 ± 0.05	1.5 ± 0.04	0.46	0.70
	HA	18.0	42.4	49.0 ± 0.2	2.0 ± 0.05	0.20	0.86
	HA + BVC	17.9	43.1	41.7 ± 0.1	2.6 ± 0.06	0.70	4.99
	HA + RVC	17.9	42.3	34.0 ± 0.04	1.6 ± 0.04	3.30	32.2
30		10.5	54.1	12.4 ± 0.1	4.7 ± 0.3	48.3	$5.5{\cdot}10^3$
	BVC	10.1	63.7	13.2 ± 0.8	4.5 ± 0.3	64.1	$6.2{\cdot}10^3$
	RVC	10.3	62.8	12.8 ± 0.8	4.6 ± 0.3	53.2	$4.6{\cdot}10^3$
	HA	10.6	57.4	14.4 ± 0.3	3.3 ± 0.2	16.8	$5.1{\cdot}10^3$
	HA + BVC	10.2	59.0	10.6 ± 1.2	4.8 ± 0.3	67.9	$5.4{\cdot}10^3$
	HA + RVC	10.4	58.2	11.7 ± 0.9	4.6 ± 0.3	58.9	$5.1{\cdot}10^3$
15–15		11.3	37.3	13.16 ± 1.0	5.22 ± 0.4	67.0	$4.8{\cdot}10^3$
	BVC	10.8	41.5	13.93 ± 0.8	4.78 ± 0.3	89.9	$4.4{\cdot}10^3$
	RVC	10.9	39.9	13.92 ± 0.8	4.72 ± 0.3	74.1	$4.4{\cdot}10^3$
	HA	11.0	38.4	19.57 ± 0.2	3.06 ± 0.2	41.8	$3.7{\cdot}10^3$
	HA + BVC	10.7	38.0	19.58 ± 0.2	3.46 ± 0.2	45.5	$3.9{\cdot}10^3$
	HA + RVC	10.8	38.1	19.36 ± 0.20	3.14 ± 0.16	45.44	$3.96{\cdot}10^3$

Note: Ratio G'/G" and viscosity η are parameters measured at 37 °C (n = 3/formulation). Additives concentrations were: 0.5 % BVC or RVC and 1 % for HA.

modynamic parameters can help assess the stability and micellization processes for hydrogel formation. It is expected that highly concentrated hydrogels or some complex systems (such as polymeric blends, the addition of salts, drugs, and other polymers) would exhibit low micellization temperatures as a strategy to minimize the free energy in the system [33,35,36]. Some representative thermograms are displayed on Supplementary Material.

In the present study, both BVC and RVC affected the structuring of hydrogel, increasing system enthalpy. An enhanced enthalpy value indicates that BVC and RVC can induce PL chain interactions (evoking polymer self-assembly). Considering that both drugs are in salt form, the system tends to be dehydrated owing to the movement of water molecules from the PPO core in the direction of the PEO blocks present in boundaries [36]. In addition, as BVC (log P = 798) is more hydrophobic than RVC (log P = 592) [1], the micellization temperature decreased, especially for the binary system (from 11.3 °C in BP to 10.8 °C in BP + BVC), while increasing enthalpy (from 37.3 kJ/mol in BP to 41.5 kJ/mol in BP + BVC). Additionally, as HA is a highly hydrophilic polymer, it could impact system structuring, as observed by SANS analysis, owing to the increased enthalpy values observed for all formulations (42.4 kJ/mol in P15 + HA, 57.4 kJ/mol in P30 + HA, and 38.4 kJ/mol in BP + HA).

3.3. Rheological studies: drugs, poloxamer type, and HA shifted the sol–gel transition and improved viscoelastic properties of formulated hydrogels

The sol–gel transition temperature (Tsol-gel) is one of the main properties to be considered for developing thermosensitive pharmaceutical formulations, as polymer concentration, drugs, and salt incorporation can modulate hydrogel formation and mechanical properties [2,33,37]. Therefore, thermosensitive formulations should be available in the sol state for better handling or injection, whereas the gel state affords requisite conditions for sustained drug release [2,9,38]).

Intermolecular interactions among various structures in the system, which are affected by the presence of additives, can interfere with the behavior of materials under different physical conditions. Tsol-gel decreases as a function of the final polymer concentration, owing to the greater probability of polymer–polymer interactions [20,33]. Likewise, BP formulations displayed low Tsol-gel values at higher PL concentrations, demonstrating a linear PL concentration-dependent behavior for the PL examined in the present study. Conversely, Tsol-gel for BP PL407 15 % + PL338 15 % approximated the value obtained for PL407 30 % (approximately 13 °C); therefore, the hydrophilic character of PL338 (Table 1, Fig. 5) at low concentrations did not impact the gelation process, as previously reported [9].

The presence of HA slightly affected the gelation temperature of hydrogels composed of PL, which was altered from 12.4 to 14.4 °C in the P30 + HA formulation. Nevertheless, HA interferes with the gelation process of the binary system, probably due to the hydrophilic interaction between HA hydroxyl radicals and the PEO block of the PL338 structure, given that lower entropy values were observed for the BP + HA formulation than the BP formulation, as shown by DSC results.

The incorporation of both BVC and RVC altered the structural organization of hydrogels, as well as their responsiveness to temperature variation (Fig. 5). In the hydrochloride form, BVC and RVC increased the interactions between PL407 and PL338 unimers, resulting in lower Tsol-gel values following salting-out due to the Hoffmeister effect [39,40]. This indicated that the presence of specific ions could disturb the aggregation state by promoting increased interactions between polymeric chains.

For P15 + HA formulations, the drug influence was more pronounced, as the addition of RVC induced a sol–gel shift from ~ 49 to 34 °C. Although BVC or RVC did not significantly alter Tsol-gel in PL407 30 % systems (Tsol-gel ~ 13° C), both drugs tended to decrease Tsol-gel of P30 + HA systems. Furthermore, HA incorporated into PL407 15 % + PL338 15 % led to a shift in Tsol-gel values from 13 to 20 °C (Fig. 5, Table 1).

In general, PL-based hydrogels tend to exhibit elastic behavior or a more rigid state at high polymer concentrations, as observed by the G' (elastic modulus)/G'' (viscous modulus) ratio (Table 1). This parameter can be influenced by hydrophilic and hydrophobic interactions among polymeric chains and is altered in the presence of additives in formulations.

Above a 15 % PL concentration, the hydrogel stiffness increased with increasing temperature (for P30, for example, G'/G"~42- and 48-times at 25 and 37 °C, respectively), owing to the progressive dehydration of PEO blocks. The increased G' values observed for BP samples (G'/G'' = 67 at 37 °C) suggested that the hydrogen bonds between PEO blocks of PL38 chains are stronger than those observed in PEO chains of PL407.

In contrast, HA insertion could decrease the G'/G'' relationship and hydrogel viscoelastic properties. The enhanced hydration capacity induced by HA incorporation, and subsequent water

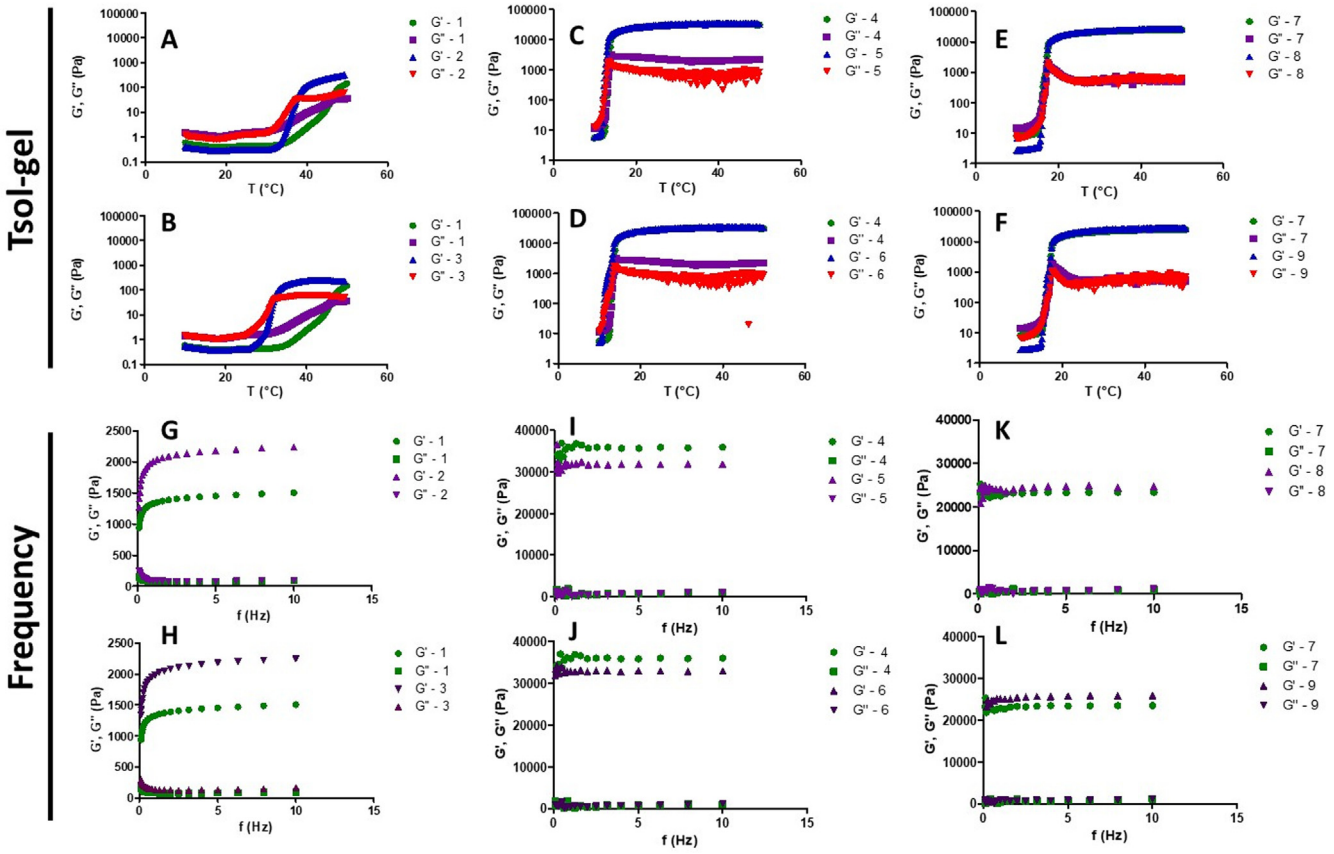

Fig. 5. G' and G'' moduli as a function of temperature and frequency variation for P15, P30 and BP formulations. As expected, P30 and BP samples have lower sol–gel transition temperature than P15 ones. The incorporation of hyaluronic acid (HA), bupivacaine (BVC) or ropivacaine (RVC) did not change the materials stability against oscillatory variation. (1) P15 + HA, (2) P15 + HA + BVC, (3) P15 + HA + RVC, (4) P30 + HA, (5) P30 + HA + BVC, (6) P30 + HA + RVC, (7) BP + HA, (8) BP + HA + BVC, (9) BP + HA + RVC. Graphs are represented as comparative analysis, as follows: A- 1 and 2; B- 1 and 3; C-4 and 5; D- 4 and 6; E- 7 and 8; F- 7 and 9 for Tsol-gel analysis; G- 1 and 2; H- 1 and 3; *I*-4 and 5; J- 4 and 6; K- 7 and 8; L- 7 and 9 for frequency sweep.

retention, reduced possible micelle-micelle interactions, impacting hydrogel stiffness. As the presence of HA in the P30 + HA formulation decreased the G'/G'' ratio by ~ 3-times when compared with P30 (from ~ 48 in P30 to ~ 17 in P30 + HA, at 37 °C), HA could exert a "linker-like" function between aqueous and polymeric interfaces, resulting in a low-viscosity material, as determined by SANS analysis and the interaction model (Fig. 4). Additionally, BP + HA rheological analysis revealed that HA exerted a polymer–polymer disaggregating role in this binary system [32]; Nascimento et al., 2013), favoring hydrophilic interactions among formulation components and decreasing hydrogel viscosity when compared with P30, P30 + HA, and BP formulations (Fig. 4), which is in line with previous studies in the literature.

For samples composed of PL407 30 % or PL407 15 % + PL 338 15 %, BVC incorporation increased G'/G'' (from 48 to 164 and from 67 to 90 in P30 + BVC and BP + BVC, respectively). Subsequently, the presence of BVC could increase interactions between polymeric chains, resulting in hydrogel rigidity. Therefore, BVC and RVC act as elements that facilitate aggregation of PL unimers, owing to the dehydration of hydrophobic PPO blocks in the micellar core. In their salt forms, both drugs can promote the expulsion of water molecules from the micelle core, thereby increasing inter-chain interactions among PL monomers. As observed, the rheological behavior of BP differs following drug incorporation into the formulation, as there is a tendency to decrease variations in viscosity, although BP binary systems are hydrogels with high viscosity (Figure S1). This can be attributed to the hydration of PL338 hydrophilic chains, as this poloxamer exhibits a higher proportion of PEO: PPO than PL407 (5:1 in PL338 and 3:1 in PL407), reflecting the higher hydrophilic-hydrophobic balance of PL338. In contrast, water molecules are potentially retained by the HA chains in the intermicellar space.

In this sense, for studying the water molecules influence into hydrogels mechanical properties, frequency sweep and viscosity analysis were also performed for comparing samples prepared in D_2O and H_2O. Comparative rheograms (frequency sweep and viscosity analysis) are presented on Figures S3 and S4 (Suppl. Mat) as well as G'/G' relationship and Tsol-gel on Table S4 (Suppl. Mat). Systems containing BVC were selected for those analysis, since most pronounced structural changes were detected by SANS analysis for those hydrogels formulations. In general, rheological properties were similar for samples prepared in H_2O and D_2O. Viscosity values were slightly decreased, compared with H_2O samples. However, the addition of D_2O seems do not change hydrogels rigidity and G'/G'' ratio parameters (Table S4), and even in presence of D_2O, rheology results are similar as in presence of H_2O (Figure S3 and S4). Tsol-gel values resulted into the same intervals (from 10 to 19 °C and 14 to 19 °C, for H_2O and D_2O, respectively), but some particular changes were observed for hydrogels containing HA + BVC (prepared in D_2O), which can possible be attributed to stronger hydrogen bonding formed by D2O and hydroxyl groups from HA or PEO. In fact, some studies in the literature have reported those structural differences by rheology and SAXS techniques for different compositions of supramolecular hydrogels [41–43], being an essential approach to compare possible experimental interferences on colloidal materials phase organization.

It should be noted that drug-delivery materials must be stable when subjected to conditions simulating physiological behaviors. Hydrogel analysis under frequency variation did not considerably alter the elastic and viscous moduli at 37 °C (physiological temperature) and low frequencies (normally between 0 and 10 Hz) [2,19,37]. All formulations showed low G' and G'' variations over the frequency range, indicating material stability. Moreover, we observed that G' was greater than G'' throughout the frequency range, indicating that the hydrogel remains in a gel state when the frequency increases; that is, the interactions between the particles are sufficiently strong to hold together and resist high shear stress conditions (Fig. 5).

The flow curves were also determined to evaluate formulation stability. However, under flow and high shear stress, such as when using a syringe for application, it is expected that the hydrogel will be organized to return to its original structural organization and consistency after injection. Otherwise, the sustained-release capability is lost [19,44–46].

Typically, hydrogels exhibited flow stability; however, the BP + RVC system showed a higher hysteresis area than that of BP + BVC, possibly due to the influence of the additive homogeneity in hydrogels [44]. Additionally, RVC incorporation promoted an increase in viscosity against flow variation. Therefore, greater destabilization of the hydrogel mechanical properties was observed following RVC incorporation than with BVC addition, as demonstrated by the higher hysteresis of RVC than that of BVC. In contrast, the highly hydrated binary system BP + HA probably presented the weakest polymer–polymer interactions. Incorporating BVC or RVC did not alter the material organization under flow variations, even when sufficiently stable to maintain the hydrogel structure after flow (Fig. 6).

The hydrogel flow properties are listed in Table 2, displaying the consistency (K) and flow index (m). Consistency is a material property that describes the resistance in response to a material undergoing an external force. This property is especially important for examining the application of formulations on mucous tissues and sensitive surfaces, that is, the importance of formulation rigidity for application. Thus, consistency is a numerical representation of the level of interaction between all components in the system. All formulations showed non-Newtonian behavior, exhibiting shear-thinning and pseudoplastic characteristics, as the flow index m was <1 [19,47]. This feature favors the utilization of these materials for pharmacological and cosmetic use, as the hydrogel can flow more easily and allow surface spreading with stress application [19]. In addition, when stress is removed, the material is organized again [19,44,45]. The consistency index K showed that P30 samples were almost 3000-times more rigid than the P15 samples (Table 2). Additionally, PL407 30 % was three-times stiffer than the binary formulation PL407 15 % + PL338 15 %, confirming the role of water in hydrogel structuring of BP systems. Conversely, the addition of HA to the P30 and BP formulations did not induce major changes in stiffness, although a slight decrease in K values was noted in the BP samples due to chain hydration.

The m values (Table 2) revealed the ability of formulation components to alter the mechanical properties of materials. As expected, the P15 hydrogels behaved as Newtonian liquids ($m \sim 1$), given the low PL concentration. P30 and BP are strictly pseudoplastic materials ($m \ll 1$); however, superior hydration affords BP samples greater fluidity than P30 samples.

Examining the adhesive properties of hydrogel systems is critical to clarifying the material's potential to be retained on a specific surface [46,47] [19] based on the analysis of G' and G'' as functions of frequency and fitting, data on the adhesion and viscosity index were obtained. As the rheological measurements were performed on a smooth surface, the results are consistent with this type of surface [19,47]. The adhesion value or gel strength A is another parameter that reflects the structural organization of the system. As shown in Table 2, adherence was mainly affected by the composition of the PL matrix and, to a lesser extent, by additives (drugs and HA). Therefore, the main elements for hydrogel structuring were the percentage and type of PL. However, RVC has a destabilizing role in the structure, decreasing the A parameter when compared with P30. In contrast, the inclusion of BVC slightly increased structural organization.

The mechanical properties of a material composed of polymeric networks can be clarified both experimentally and by modeling. The level of interactions between chains can be inferred by analyzing material behavior by frequency and using the Maxwell model [20,21].

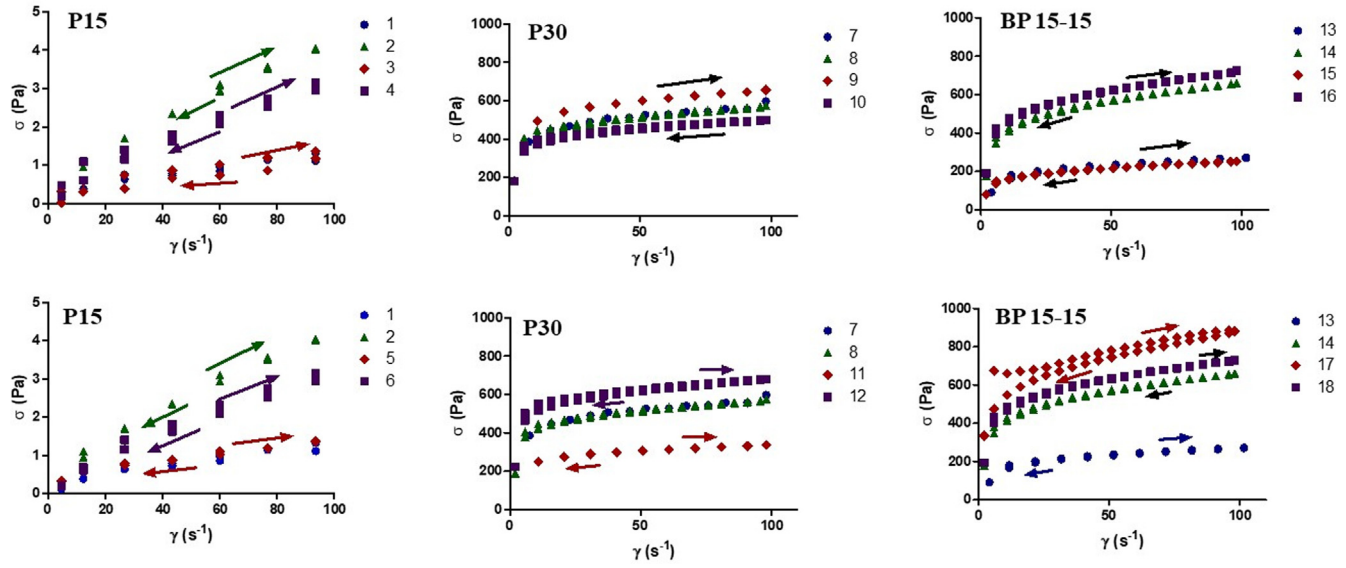

Fig. 6. Flow curves of P15, P30 and BP formulations. all formulations show structural stability when they are subjected to flow, with low hysteresis being observed. (1) P15, (2) P15 + HA, (3) P15 + BVC, (4) P15 + HA + BVC, (5) P15 + RVC, (6) P15 + HA + RVC, (7) P30, (8) P30 + HA, (9) P30 + BVC, (10) P30 + HA + BVC, (11) P30 + RVC, (12) P30 + HA + RVC, (13) BP, (14) BP + HA, (15) BP + BVC, (16) BP + HA + BVC, (17) BP + RVC, (18) BP + HA + RVC. Arrows indicate the initial and final frequency variations.

Table 2
Consistency (K) and flow index (m) of P15, P30, and BP samples at 25 °C.

Formulation	K (Pas^{-m})	m	R^2	S(Pas^{-n})	n	R^2
P15	0.14 ± 0.02	0.94 ± 0.02	0.9953	1340 ± 32.5	0.107 ± 0.009	0.8841
P15 + BVC	0.38 ± 0.03	0.76 ± 0.02	0.9929	1546 ± 35.6	0.101 ± 0.009	0.8805
P15 + RVC	0.16 ± 0.01	0.82 ± 0.01	0.9999	1134 ± 30.9	0.107 ± 0.010	0.8563
P15 + HA	0.38 ± 0.02	0.80 ± 0.01	0.9969	1101 ± 16.4	0.084 ± 0.006	0.9199
P15 + HA + BVC	0.27 ± 0.03	0.83 ± 0.02	0.9927	1608 ± 36.3	0.093 ± 0.009	0.8645
P15 + HA + RVC	0.34 ± 0.03	0.83 ± 0.01	0.9955	1606 ± 29.3	0.092 ± 0.007	0.9049
P30	306.6 ± 6.5	0.140 ± 0.004	0.9856	31342 ± 468.3	0.017 ± 0.005	0.5714
P30 + BVC	368.7 ± 4.9	0.128 ± 0.003	0.9923	31857 ± 362.5	0.023 ± 0.004	0.7481
P30 + RVC	185.0 ± 2.1	0.132 ± 0.003	0.9946	26925 ± 292.6	0.016 ± 0.004	0.6490
P30 + HA	302.8 ± 1.8	0.136 ± 0.002	0.9980	33283 ± 351.5	0.021 ± 0.004	0.7736
P30 + HA + BVC	268.1 ± 1.6	0.134 ± 0.002	0.9979	30538 ± 227.5	0.012 ± 0.003	0.7399
P30 + HA + RVC	378.1 ± 2.2	0.126 ± 0.002	0.9978	31999 ± 96.4	0.008 ± 0.001	0.8464
BP	98.0 ± 1.2	0.219 ± 0.003	0.9987	26976 ± 149.1	0.018 ± 0.001	0.9418
BP + BVC	95.8 ± 0.6	0.209 ± 0.002	0.9983	27141 ± 103.2	0.013 ± 0.001	0.8628
BP + RVC	348.5 ± 4.8	0.198 ± 0.003	0.9955	23702 ± 237.4	0.021 ± 0.004	0.7615
BP + HA	243.8 ± 1.9	0.216 ± 0.002	0.9989	21,987 ± 87.5	0.017 ± 0.001	0.9202
BP + HA + BVC	280.7 ± 1.7	0.203 ± 0.002	0.9992	21694 ± 283.6	0.037 ± 0.004	0.8848
BP + HA + RVC	284.1 ± 1.8	0.204 ± 0.002	0.9992	23773 ± 151.1	0.023 ± 0.002	0.8658

Table S2 shows G_∞, which, according to Maxwell's model, refers to the number of entanglements that exist in the network or the interaction between the chains [20,21]. It is proposed that G_∞ is proportional to the viscosity of the material; hence, a high value can be determined based on interactions among materials components. An increase in PL concentration enhanced interactions between both polymers: PL 15 % presented a G_∞ value of 1807 Pa, which exceeded 33.000 Pa at PL 30 %.

In contrast, the hydrophilic character of PL338 decreased the organization between the chains, owing to features such as a high hydrophilic-lipophilic balance and molecular weight when compared with PL407. Given that the PEO:PPO relationship of PL338 was greater than that of PL407 (5:1 *vs* 3:1), a relatively small decrease in G_∞ in BP formulations may indicate the presence of structures formed by both PL407 + PL338 and exclusively by PL 407 or PL 338, dispersed within the same hydrogel. Additionally, HA caused a small decrease in polymer interactions of PL407 15 % + PL338 15 %, probably via disorganization of the corona region in the BP formulation.

Regarding drug influence, RVC molecules possibly cause minimal structural disorganization, while the opposite occurs with BVC incorporation into structures, where sample components are present, favoring interaction. This effect was confirmed by the relaxation time τ in P30 gels, which was proportional to the inverse of the disengagement rate of chains. The presence of BVC in P30 increased τ from ~ 2 s to nearly 5 s; in P30 + HA, BVC addition increased τ from ~ from nearly 3 s to appromimately 8 s. The presence of a butyl group in the BVC molecule may hinder chain relaxation and consequently, the return of the polymeric matrix to its initial state [20].

3.4. In vitro drug release assays

The main purpose of drug release analysis is to examine the capacity of the hydrogel formulation to retain the drug and modulate its release into the medium [2,24,38,48,49]. Fig. 7 shows the gradual drug release concentrations. All release constant values (Krel) and their mathematical modeling are shown in Table 3.

P30 and BP samples, exhibiting higher consistency than P15, could retain BVC for a longer time than P15 + BVC. However, the presence of PL338 and HA seemed to hinder BVC release, probably due to the formation of a second polymeric matrix (composed of HA chains) within intermicellar spaces, in agreement with the results from structural studies. In addition, we observed that both P30 + HA and BP + HA controlled the release in a similar manner; however, they were more efficient than the P30 and BP formulations.

After approximately 8 h, with greater BVC concentrations detected in the medium with the P15 formulation (~1.5 mM) than with systems composed of P30 (~0.6 mM) and BP (~0.7 mM) with $p < 0.001$. Similar results were obtained for RVC-loaded systems, where P15 (~1.4 mM), P30 (~1.1 mM), and BP (~0.6 mM) distinctively modulated drug release. However, statistical differences were observed only between P30 and BP, suggesting that the polymeric composition binary system markedly impacted the reduced RVC release concentrations ($p < 0.01$).

Considering mathematical modeling data (Table 3), it was observed that drug release from hydrogels followed different mechanisms based on the PL final concentration, drug hydrophobicity, and HA insertion.

For RVC-loaded systems, in the absence of HA, the best correlation coefficients ($0.55 < R^2 < 0.98$) were obtained from the Korsmeyer-Peppas model for P15, P30, and BP formulations, with super case-II kinetics determining the contribution of both diffusion and erosion mechanisms [9,36,50]. However, BVC-loaded hydrogels followed Korsmeyer-Peppas and zero-order mathematic models, suggesting that BVC release can be modulated by the final drug concentration and polymer composition, given that P15 and P30-BVC followed zero-order and Korsmeyer-Peppas models, respectively. The higher PL407 concentration in the P30 hydrogel than in the P15 hydrogel could explain this differential drug modulation. Accordingly, the final PL concentration was maintained, but hydrophilic PL (PL338) was incorporated into the systems, promoting a modulatory behavior similar to that observed with P15.

In the presence of HA, drug release profiles were not homogeneous. Different release mechanisms were observed, with drug diffusion predominant over erosion mechanisms. Although cubic and hexagonal phase organizations were maintained in the hydrogels before and after HA, their incorporation reduced both BVC and RVC Krel values, indicating that their presence plays an important role in modulating drug release by diffusion and/or erosion mechanisms. Similar results were also reported by Nascimento and coworkers (2018) [9] for PL-based systems containing lidocaine base with low HA concentrations (0.05 %) when compared with systems reported in the present study (0.5 %).

It can be speculated that formulations with considerably organized structures best control the output of molecules. Drugs are incorporated into micelles even at temperatures below the gela-

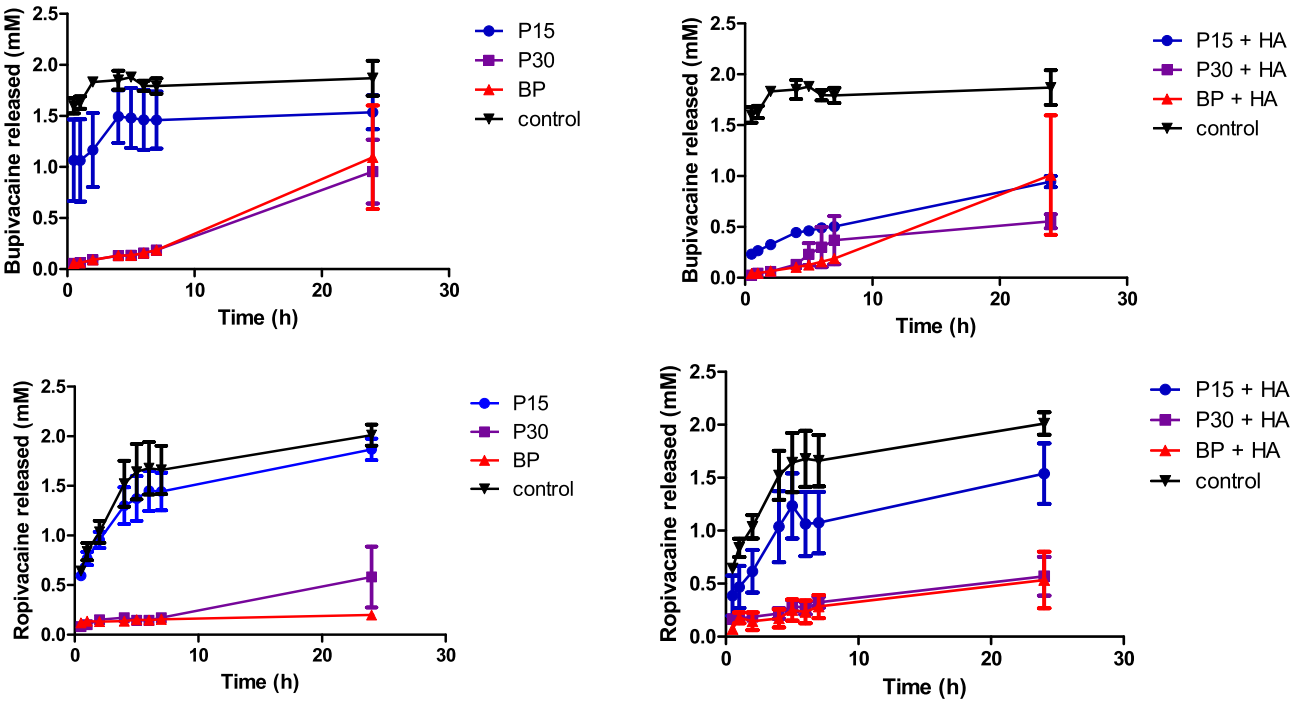

Fig. 7. Drug release profiles for P15, P30 and BP formulations containing bupivacaine (BVC) and ropivacaine (RVC). As expected, samples with high concentration of poloxamer present much augmented release control than lower concentrated formulation (n = 6/ formulation). Controls refer to BVC or RVC solutions (0.5 % m/v in ultrapure water).

Table 3
Release constants and determination coefficients for BVC or RVC from differente hydrogels formulations.

	Higuchi model		Zero-order model		Korsmeyer-Peppas model		
	K_h	R^2	K_0	R^2	K_k	n	R^2
BVC	0.32 ± 0.02	0.789	0.51 ± 0.09	0.65	nd	nd	nd
RVC	0.45 ± 0.09	0.789	0.62 ± 0.10	0.58	nd	nd	nd
P15 + RVC	–	–	0.08 ± 0.01	0.8117	0.037 ± 0.0001	0.29 ± 0.03	0.9247
P30 + RVC	0.23 ± 0.007	0.9487	0.104 ± 0.004	0.9671	0.010 ± 0.001	0.82 ± 0.03	0.9822
BP + RVC	0.21 ± 0.02	0.8521	0.026 ± 0.003	0.8609	0.010 ± 0.002	0.77 ± 0.03	0.9446
P15 + HA + RVC	–	–	0.017 ± 0.004	0.8981	0.015 ± 0.001	0.35 ± 0.04	0.8741
P30 + HA + RVC	0.18 ± 0.03	0.9468	0.069 ± 0.011	0.6789	0.007 ± 0.003	0.89 ± 0.15	0.6549
BP + HA + RVC	0.14 ± 0.02	0.9629	0.030 ± 0.002	0.9253	0.012 ± 0.001	0.45 ± 0.03	0.9477
P15 + BVC	0.68 ± 0.04	0.6680	0.16 ± 0.030	0.6733	0.011 ± 0.007	0.20 ± 0.05	0.5918
P30 + BVC	0.04 ± 0.018	0.5733	0.083 ± 0.006	0.7733	0.009 ± 0.002	0.77 ± 0.09	0.9077
BP + BVC	0.20 ± 0.04	0.8466	0.018 ± 0.002	0.8930	0.011 ± 0.0003	0.73 ± 0.03	0.7554
P15 + HA + BVC	0.150 ± 0.005	0.6262	0.029 ± 0.001	0.9437	0.014 ± 0.001	0.42 ± 0.02	0.9540
P30 + HA + BVC	0.130 ± 0.005	0.9262	0.051 ± 0.005	0.8534	0.011 ± 0.003	0.64 ± 0.04	0.8272
BP + HA + BVC	0.093 ± 0.011	0.4233	0.036 ± 0.007	0.4996	0.006 ± 0.003	0.69 ± 0.04	0.8826

Note: data are expressed as mean ± standard deviation (n = 6/ formulation). Nd- non determined since no correlation was found.

tion temperature, and above this limit, the drugs are retained in intermicellar spaces, especially considering drugs available in salt forms, such as BVC and RVC hydrochloride.

Based on diffusion coefficients, a high PL concentration reduced molecular diffusion, which was potentially attributed to entanglement (Table S5). The diffusion of RVC molecules through these systems was faster than that in BVC-composed hydrogels. As expected, RVC molecules could diffuse more easily than BVC molecules, given their hydrophilic character. Drug release profiles and calculated diffusion coefficients revealed that high poloxamer concentrations blocked drug release, owing to the highly packed arrangements of PL matrixes with a diminished number and size of water channels [6,51]. These robust intermolecular interactions in the PL chains increased the viscosity response to altering temperature; however, more hydrophilic components tend to decrease this response and block drug diffusion. Additionally, FTIR results suggested that PL interactions could be affected by hydrogen bonds between the ether oxygen (C—O—C) and amine and amide groups of BVC [6], thereby facilitating intermolecular interactions and consequently reducing the sol–gel transition temperature [6,9,51], confirming our findings.

4. Conclusions

In the present study, we aimed to examine and characterize PL-based hydrogels to control local anesthetic release and determine the required structural organization for promising sustained drug release profiles. The polymer matrix concentration and physicochemical properties could influence both the supramolecular structure and drug release mechanisms of hydrogels.

Based on the structural analysis, we established the formation of a mixed hydrogel and that both polymers exhibited distinct molecular masses and hydrophilicities. In addition, different phase organizations were found to coexist, with both cubic and hexagonal phase organizations identified. Regarding drug incorporation, hydrogels with the highest PL concentrations were more sensitive to the presence of RVC than to BVC, causing a disturbance in micelle-micelle interactions. However, this effect was absent after HA incorporation, suggesting its location in the intermicellar spaces probably interacting with the hydrophilic corona, thereby allowing structural stabilization via hydrophilic interactions between hydroxyl groups and PEO blocks from HA and PL, respectively. Indeed, the formation of a more hydrated system induced by HA incorporation reduced the micelle-micelle interactions, impacting hydrogel stiffness, as observed by rheological analysis. In addition, the presence of BVC increased the interactions between polymeric chains, thereby affecting hydrogel rigidity. Therefore, BVC and RVC facilitate the aggregation of PL unimers due to the dehydration of hydrophobic PPO blocks into the micellar core.

These structural features were essential to elucidate the drug release mechanisms, with a predominance of diffusion over erosion mechanisms detected. Cubic and hexagonal phase organizations were maintained in hydrogels before and after HA addition; however, HA incorporation reduced both BVC and RVC release constant values, indicating that its presence plays an important role in modulating drug release, despite considering both phase organizations. This presents a wide potential for manipulation for designing and planning drug-delivery materials with distinct properties, such as thermosensitivity (poloxamers) and high biocompatibility (HA), modulated by their internal phase organization.

In special, this work reveals a new look to those structural requirements comparing the hydrogels performance according to both polymeric composition and two chemically related drugs, showing that even considering their similarities (chemical structure, physico-chemical properties, and clinically available dosage forms), drugs can modulate their incorporation into different hydrogels phases, such as micellar core or intermicellar spaces (in the case of hexagonal phase organization). Additionally, the presence of hyaluronic acid enhances the systems hydrophilicity (due to its numerous hydroxyl groups) and the capability to carry high amounts of drug. Then, the formulations proposed here presents important vantages in physiological medium: i) the slow hydrogel dissolution and possible drug controlled release at the site of action adjacencies (such as peripheral nerves or spinal cord surroundings); ii) the high drug solubility into the hydrogels, facilitating the drug diffusion across the system; iii) the hydrogels easily dispersion when in contact with the dissolution medium, which possibly simulates the dissolution into the interstitial biological liquids.

Funding sources

The Sao Paulo Research Foundation - FAPESP (Grant 2014/14457-5, 2019/20303-4), National Council for Scientific and Technological Development - CNPq (Grant 309207/ 2016-9, 307718/2019-0). This study was also supported by The Coordenação de Aperfeiçoamento de Pessoal de Nível Superior—Brasil (CAPES)—Finance Code 001.

Authorship contribution statement

AFS performed the conception, structural analysis and wrote the manuscript. MKV, FY, MKKDF and DRA contributed to the design, data analysis, review and wrote the manuscript.

Data availability

Data will be made available on request.

Declaration of Competing Interest

The authors declare the following financial interests/personal relationships which may be considered as potential competing interests: [Anderson Ferreira Sepulveda reports financial support was provided by Coordination of Higher Education Personnel Improvement. Daniele Ribeiro de Araujo reports financial support was provided by State of Sao Paulo Research Foundation. Daniele Ribeiro de Araujo reports was provided by National Council for Scientific and Technological Development. Anderson Ferreira Sepulveda has patent Micellar Supramolecular Structure Software (MiSS) issued to BR512021000746-8. Not applied].

Appendix A. Supplementary material

Supplementary data to this article can be found online at https://doi.org/10.1016/j.jcis.2022.10.064.

References

[1] D.R. de Araujo, L.N.M. Ribeiro, E. de Paula, Lipid-based carriers for the delivery of local anesthetics, Expert Opinion on Drug Delivery 16 (2019) 701–714, https://doi.org/10.1080/17425247.2019.1629415.
[2] A.F. Sepulveda, R. Borges, J. Marchi, D.R. de Araujo, Biomedical applications of stimuli-responsive hydrogels, in: J.K. Patra, L.F. Fraceto, G. Das, E.V.R. Campos (Eds.), Green Nanoparticles: Synthesis and Biomedical Applications, Springer, 2020, pp. 1–20, https://doi.org/10.1007/978-3-030-39246-8_1.
[3] A.M. Bodratti, P. Alexandridis, Formulation of poloxamers for drug delivery, J. Funct. Biomater. 9 (2018) 1–24, https://doi.org/10.3390/jfb9010011.
[4] R.K. Thapa, F. Cazzador, K.G. Grønlien, H.H. Tønnesen, Effect of curcumin and cosolvents on the micellization of Pluronic F127 in aqueous solution, Colloids Surf. B 195 (2020), https://doi.org/10.1016/j.colsurfb.2020.111250.
[5] J.M. White, M.A. Calabrese, Impact of small molecule and reverse poloxamer addition on the micellization and gelation mechanisms of poloxamer hydrogels, Colloids Surf. A 638 (2022).
[6] H. Abdeltawab, D. Svirskis, B.J. Boyd, A. Hill, M. Sharma, Injectable thermoresponsive gels offer sustained dual release of bupivacaine hydrochloride and ketorolac tromethamine for up to two weeks, Int. J. Pharm. 604 (2021).
[7] M.K.K.D. Franco, A.F. Sepulveda, A.A. Vigato, A. Oshiro, I.P. Machado, B. Kent, D. Clemens, F. Yokaichiya, D.R. de Araujo, Supramolecular structure of temperature-dependent polymeric hydrogels modulated by drug incorporation, ChemistrySelect 5 (2020) 12853–12861, https://doi.org/10.1002/slct.202001116.
[8] A.A. Vigato, I.P. Machado, M. del Valle, P.A. da Ana, A.F. Sepulveda, F. Yokaichiya, M. Franco, M.K.K. D, M.C. Loiola, G.R. Tófoli, C.M.S. de Cereda, M. I. de Sairre, D.R. de Araujo, Monoketonic curcuminoid-lidocaine co-delivery using thermosensitive organogels: from drug synthesis to epidermis structural studies, Pharmaceutics 14 (2022).
[9] M.H.M. Nascimento, M.K.K.D. Franco, F. Yokaichyia, E. de Paula, C.B. Lombello, C. B, D.R. de Araujo, Hyaluronic acid in Pluronic F-127/F-108 hydrogels for postoperative pain in arthroplasties: influence on physico-chemical properties and structural requirements for sustained drug-release, Int. J. Biol. Macromol. 111 (2018) 1245–1254, https://doi.org/10.1016/j.ijbiomac.2018.01.064.
[10] M.H.M. Nascimento, F.N. Ambrosio, D.C. Ferraraz, H. Windisch-Neto, S.M. Querobino, M. Nascimento-Sales, M.A. Alberto-Silva, K.K.D. Franco, B. Kent, F. Yokaichiya, C.B. Lombello, D.R. de Araujo, Sulforaphane-loaded hyaluronic acid-poloxamer hybrid hydrogel enhances cartilage protection in osteoarthritis models, Mater. Sci. Eng. C (2021) 128, https://doi.org/10.1016/j.msec.2021.112345.
[11] S.M. Querobino, N.C. de Faria, A.A. Vigato, B.G.M. da Silva, I.P. Machado, M.S. Costa, F.N. Costa, D.R. de Araujo, C. Alberto-Silva, Sodium alginate in oil-poloxamer organogels for intravaginal drug delivery: Influence on structural parameters, drug release mechanisms, cytotoxicity and in vitro antifungal activity, Mater. Sci. Eng.: C 99 (2019), https://doi.org/10.1016/j.msec.2019.02.036.
[12] H. Abdeltawab, D. Svirkis, M. Sharma, Formulation strategies to modulate drug release from poloxamer based in situ gelling systems, Expert Opin. Drug Del. 17 (2020), https://doi.org/10.1080/17425247.2020.1731469.
[13] G. Kogan, L. Šoltés, R. Stern, P. Gemeiner, Hyaluronic acid: a natural biopolymer with a broad range of biomedical and industrial applications, Biotechnol. Lett. 29 (2007) 17–25, https://doi.org/10.1007/s10529-006-9219-z.
[14] T. Iannitti, D. Lodi, B. Palmieri, Intra-articular injections for the treatment of osteoarthritis: focus on the clinical use of hyaluronic acid, Drugs R.D 11 (2011) 13–27.
[15] B. Hammouda, SANS from Pluronic P85 in d-water, Eur. Polym. J. 46 (2010) 2275–2281, https://doi.org/10.1016/j.eurpolymj.2010.10.012.

[16] E. Törnquist, L. Gentile, S. Prévost, A. Diaz, U. Olsson, H. Isaksson, Comparison of small-angle neutron and X-ray scattering for studying cortical bone nanostructure, Sci. Rep. 10 (2020).
[17] L. Donina, A. Rafique, S. Khodaparast, L. Porcar, J.T. Cabral, Lamellar-to-MLV transformation in SDS/octanol/brine examined by microfluidic-SANS and polarized microscopy, Soft Matter 17 (2021) 10053–10062.
[18] E. Csapó, H. Szokolai, Á. Juhász, N. Varga, L. Janovák, I. Dékány, Cross-linked and hydrophobized hyaluronic acid-based controlled drug release systems, Carbohydr. Polym. 195 (2018).
[19] F.D. Victorelli, G.M.F. Calixto, M.A.S. Ramos, T.M. Bauab, M. Chorilli, Metronidazole-loaded polyethyleneimine and chitosan-based liquid crystalline system for treatment of Staphylococcal skin infections, Biomed. Nanotechnol. 14 (2018) 227–237, https://doi.org/10.1166/jbn.2018.2484.
[20] T. Annable, R. Buscall, R. Ettelaiee, D. Whittlestone, The rheology of solutions of associating polymers: comparison of experimental behavior with transient network theory, J. Rheol. 37 (1993) 695–726, https://doi.org/10.1122/1.550391.
[21] M. Abrami, I. D'Agostino, G. Milcovich, S. Fiorentino, R. Farra, F. Asaro, R. Lapasin, G. Grassi, M. Grassi, Physical characterization of alginate-Pluronic F127 gel for endoluminal NABDs delivery, Soft Matter 10 (2014) 729–737, https://doi.org/10.1039/c3sm51873f.
[22] M.S. Green, A.V. Tobolsky, A new approach to the theory of relaxing polymeric media, J. Chem. Phys. 14 (1946) 80–89.
[23] A.C.S. Akkari, J.Z.B. Papini, G.K. Garcia, M.K.K.D. Franco, L.P. Cavalcanti, A. Gasperini, M.I. Alkschbirs, F. Yokaichyia, E. de Paula, G.R. Tófoli, D.R. de Araujo, Poloxamer 407/188 binary thermosensitive hydrogels as delivery systems for infiltrative local anesthesia: Physico-chemical characterization and pharmacological evaluation, Mater. Sci. Eng., C 68 (2016) 299–307, https://doi.org/10.1016/j.msec.2016.05.088.
[24] P. Costa, J.M.S. Lobo, Modeling and comparison of dissolution profiles, Eur. J. Pharm. Sci. 13 (2001) 123–133.
[25] M.L. Veyries, G. Couarraze, S. Geiger, F. Agnely, L. Messias, B. Kunzli, F. Faurisson, B. Rouveix, Controlled release of vancomycin from Poloxamer 407 gels, Int. J. Pharm. 192 (1999) 183–193.
[26] G. González-Gaitano, C. Müller, A. Radulescu, C.A. Dreiss, Modulating the self-assembly of amphiphilic X-shaped block copolymers with cyclodextrins: structure and mechanisms, Langmuir 31 (2015) 4096–4105, https://doi.org/10.1021/acs.langmuir.5b00334.
[27] G. González-Gaitano, M.A. da Silva, A. Radulescu, C.A. Dreiss, Selective tuning of the self-assembly and gelation of a hydrophilic poloxamine by cyclodextrins, Langmuir 31 (2015) 5645–5655, https://doi.org/10.1021/acs.langmuir.5b01081.
[28] R.A. Bini, M.F. Silva, L.C. Varanda, M.A. da Silva, C.A. Dreiss, Soft nanocomposites of gelatin and poly(3-hydroxybutyrate) nanoparticles for dual drug release, Colloids Surf. B 157 (2017) 191–198, https://doi.org/10.1016/j.colsurfb.2017.05.051.
[29] R. Ivanova, B. Lindman, P. Alexandridis, Modification of the lyotropic liquid crystalline microstructure of amphiphilic block copolymers in the presence of copolymers, Adv. Colloid Interface Sci. 89 (2001) 351–382.
[30] I.W. Hamley, J.A. Pople, J.P.A. Fairclough, A.J. Ryan, C. Booth, Y.W. Yang, Shear-induced orientational transitions in the body-centered cubic phase of a deblock copolymer gel, Macromolecules 31 (1998) 3906–3911, https://doi.org/10.1021/ma971561m.
[31] N. Jindal, S.K. Mehta, Nevirapine loaded Poloxamer 407/Pluronic P123 mixed micelles: Optimization of formulation and in vitro evaluation, Colloids Surf B Biointerfaces 129 (2015) 100–106, https://doi.org/10.1016/j.colsurfb.2015.03.030.
[32] L. Mayol, F. Quaglia, A. Borzacchiello, L. Ambrosio, M.I. La Rotonda, A novel poloxamer/hyaluronic acid in situ forming hydrogel for drug delivery: Rheological, mucoadhesive and in vitro release properties, Eur. J. Pharm. Biopharm. 70 (2008) 199–206, https://doi.org/10.1016/j.ejpb.2008.04.025.
[33] A. Cabana, A. Aït-Kadi, J. Juhász, Study of gelation process of polyethylene oxide$_a$-polypropylene oxide$_b$-polyethylene oxide$_a$ copolymer (poloxamer 407) aqueous solutions, J. Colloid Interface Sci. 190 (1997) 307–312.
[34] D.C. Pozzo, K.R. Hollabaugh, L.M. Walker, Rheology and phase behavior of copolymer-templeted nanocomposite material, J. Rheol. 49 (2005) 759–782, https://doi.org/10.1122/1.1888665.
[35] A. Oshiro, D.C. da Silva, J.C. de Mello, V.W.R. de Moraes, L.P. Cavalcanti, M.K.K. D. Franco, M.I. Alkschbirs, L.F. Fraceto, F. Yokaichyia, T. Rodrigues, D.R. de Araujo, Pluronics F-127/L-81 binary hydrogels as drug-delivery systems: Influence of physicochemical aspects on release kinetics and cytotoxicity, Langmuir 30 (2014) 13689–13698.
[36] A.C.M. dos Santos, A.C.S. Akkari, I.R. Ferreira, C.R. Maruyama, M. Pascoli, V. A. Guilherme, E. de Paula, L.F. Fraceto, R. de Lima, P.S. Melo, D.R. de Araujo, Poloxamer-based binary hydrogels for delivering tramadol hydrochloride: sol-gel transition studies, dissolution-release kinetics, in vitro toxicity, and pharmacological evaluation, Int. J. Nanomedicine 10 (2015) 2391–2401.
[37] C. Pradal, K.S. Jack, L. Grøndahl, J. Cooper-White, Gelation kinetics and viscoelastic properties of pluronic and α-cyclodextrin-based pseudopolyrotaxane hydrogels, Biomacromolecules 14 (2013) 3780–3792, https://doi.org/10.1021/bm401168h.
[38] K.C.F. Mariano, J.Z.B. Papini, N.C. de Faria, D.N.C. Heluany, A.L.L. Botega, C.M.S. Cereda, E. de Paula, G.R. Tófoli, D.R. de Araujo, Ropivacaine-loaded Poloxamer binary hydrogels for prolonged regional anestesia: structural aspects, biocompatibility, and pharmacological evaluation, Biomed. Res. Int. (2021) 7300098.
[39] T.B. Becher, C.B. Braga, D.L. Bertuzzi, M.D. Ramos Junior, A. Hassan, F. N. Crespilho, C. Ornelas, The structure-property relationship in LAPONITE® materials: from Wigner glasses to strong self-healing hydrogels formed by non-covalent interactions, Soft Matter 15 (2019) 1278–1289.
[40] M. Hua, S. Wu, Y. Ma, Y. Zhao, Z. Chen, I. Frenkel, J. Strzalka, H. Zhou, X. Zhu, X. He, Strong though hydrogels via the synergy of freeze-casting and salting out, Nature 590 (2021).
[41] D. Oakenfull, A. Scott, Gelatin gels in deuterium oxide, Food Hydrocolloids 17 (2003) 207–210.
[42] M.V.C. Cardoso, E. Sabadini, The gelling of κ-carrageenan in light and heavy water, Carbohydr. Res. 345 (2010) 2368–2373.
[43] K. McAulay, H. Wang, A.M. Fuentes-Caparrós, L. Thomson, N. Khunti, N. Cowieson, H. Cui, A. Seddon, D.J. Adams, Isotopic control over self-assembly in supramolecular gels, Langmuir 36 (2020) 8626–8631.
[44] J. Mewis, N.J. Wagner, Thixotropy, Adv. Colloid Interface Sci. 147 (2009) 214–227, https://doi.org/10.1016/j.cis.2008.09.005.
[45] J.J. Xuan, P. Balakrishnan, D.H. Oh, W.H. Yeo, S.M. Park, S.M., C.S. Yong, H.G. Choi, Rheological characterization and in vivo evaluation of thermosensitive poloxamer-based hydrogel for intramuscular injection of piroxicam 395 (2010) 317 323.
[46] G. Calixto, A.C. Yoshii, H. Rocha e Silva, B.S.F. Cury, M. Chorilli, Polyacrylic acid polymers hydrogels intended to topical drug delivery: preparation and characterization, Pharm. Dev. Technol. (2014) 1–7.
[47] M.J. Lucero, J. García, J. Vigo, M.J. León, A rheological study of semisolid preparations of Eudragit®, Int. J. Pharm. 116 (1995) 31–37.
[48] S. Nie, W.L.W. Hsiao, W. Pan, Z. Yang, Thermoreversible Pluronic® F127-based hydrogel containing liposomes for the controlled delivery of paclitaxel: in vitro drug release, cell cytotoxicity, and uptake studies, Int. J. Nanomed. 6 (2011) 151–166.
[49] R. Machín, J.R. Isasi, I. Vélaz, Hydrogel matrices containing single and mixed natural cyclodextrins. Mechanisms of drug release, Eur. Polym. J. 49 (2013) 3912–3920, https://doi.org/10.1016/j.eurpolymj.2013.08.020.
[50] N.A. Peppas, Y. Huang, M. Torres-Lugo, J.H. Ward, J. Zhang, Physicochemical foundations and structural design of hydrogels in medicine and biology, Annu. Rev. Biomed. Eng. 2 (2000) 9–29.
[51] T. Irimia, G.C. Muşat, R.M. Prisada, M.V. Ghica, C.E. Dinu-Pîrvu, V. Anuţa, B.Ş. Valescu, L. Popa, Contributions on formulation and preliminar evaluation of ocular colloidal systems of chitosan and Poloxamer 407 with bupivacaine hydrochloride, Farmacia 67 (2019).